bioRxiv preprint doi: https://doi.org/10.1101/2024.07.28.605507; this version posted August 6, 2024. The copyright holder for this preprint (which was not certified by peer review) is the author/funder, who has granted bioRxiv a license to display the preprint in perpetuity. It is made available under aCC-BY-NC-ND 4.0 International license.

Supplemental Figure 1. Transposon insertions are biased regionally and by selection. A) Transposon insertion count is plotted across chromosomes. There are clear peaks at the rDNA array on Chromosome 2 and the *URA5* locus on Chromosome 8, as well as the surrounding chromosome. B) Transposon insertion count is plotted across the 2000 bases immediately upstream and downstream of the start codon. Rows are split based on predicted gene essentiality. C) Insertions per base are plotted for genes not present vs present in the deletion collection. Boxplots show first quartile, median, third quartile. The whiskers show the range to a maximum of 1.5 times the interquartile range above and below the first and third quartile, respectively. Outliers are displayed as individual datapoints.

bioRxiv preprint doi: https://doi.org/10.1101/2024.07.28.605507; this version posted August 6, 2024. The copyright holder for this preprint (which was not certified by peer review) is the author/funder, who has granted bioRxiv a license to display the preprint in perpetuity. It is made available under aCC-BY-NC-ND 4.0 International license.

Supplemental Figure 2. PCR validation of predicted essential genes with strains in deletion collection. A) Schematic of PCR validation strategy for deletions. WT alleles should be detectable with an in-gene PCR that amplifies wildtype DNA sequence (left). Mutant alleles should have the wildtype allele replaced with a drug resistance marker. The junctions between the genomic sequence and the resistance marker should be detectable via PCR on both the 5' and 3' ends (right). A successful mutant should produce bands from the 5' junction and 3' junction but not from the in-gene PCR. A wildtype strain should produce a band only from the in-gene PCR. B) PCR validations for 5 independent colonies from the deletion collection strain for CNAG_05292. All five produce wildtype in-gene bands and no junction bands. C) PCR validations for 5 independent colonies from the deletion collection strain for CNAG_06887. All five produce wildtype in-gene bands and no junction bands. D) PCR validations for deletion collection strains for CNAG_04763, CNAG_00996, CNAG_02190. All three strains produce negative in-gene PCRs and successful junction PCRs for both 5' and 3' ends.

Supplemental Figure 3. Some incorrectly predicted essential genes have growth defects in transposase inducing conditions. A) Spot dilution assays with 5 μL spots plated. The initial leftmost spot is of OD_{600} = 20 culture and each successive spot is a 10-fold dilution, so that the final spot should be 10^5 less concentrated than the first. All four plates were spotted on the same day with the same dilution series. B) Competition assay with percentage of mutant plotted on the y-axis. Each mutant was competed against the same unmarked wildtype KN99 parental strain. Strains were competed in the SC-URA+Gal media used in the original assay. Strains were originally mixed at a 50:50 ratio based on OD_{600}. Inconsistency with mixing of CNAG_00996 suggests an altered OD_{600} to CFU ratio. C) Picture of colonies on YPD plates from the competition assay for the *cnag_00996*Δ mutant. Colonies were distinctly different in appearance

bioRxiv preprint doi: https://doi.org/10.1101/2024.07.28.605507; this version posted August 6, 2024. The copyright holder for this preprint (which was not certified by peer review) is the author/funder, who has granted bioRxiv a license to display the preprint in perpetuity. It is made available under aCC-BY-NC-ND 4.0 International license.

and replica plating to YPD+NAT media confirmed that rough colonies were the mutant strain. Panel on right is zoomed in from inset box on left and is adjusted to help visualize difference between colonies more clearly.

Supplemental Figure 4. Concentration dependent inhibition of growth by fluconazole in YPD liquid. Growth at 24 hours plotted relative to a no drug control. X axis displays concentration of fluconazole added in DMSO. Y axis shows OD_{600} normalized to OD_{600} of no drug control.

Supplemental Figure 5. Shiny app allows visualization of data on publicly available website. Screenshot of a publicly available interactive Shiny app (https://bbillmyre.shinyapps.io/Crypto_TN_seq_viewer/) that visualizes data from the *Cryptococcus neoformans* TN-seq assay. There are four plots, displaying the distribution of fold changes within a gene compared with intergenic inserts (as in figure 4C,) the distribution of insert frequencies across a gene at three different experimental stages, transposon insertion frequencies across a gene with an additional 300 bases before the ATG and after the stop codon, and finally a volcano plot (as in figure 4B) with the current gene highlighted in black. The app only accepts *C. neoformans* systematic names (ie., CNAG_0####).

Supplemental Table 1. Table containing essentiality predictions and fluconazole response data.

Supplemental Table 2. Table containing GO predictions for predicted essential genes lacking predicted human orthologs

Supplemental Table 3. Strain table.

bioRxiv preprint doi: https://doi.org/10.1101/2024.07.28.605507; this version posted August 6, 2024. The copyright holder for this preprint (which was not certified by peer review) is the author/funder, who has granted bioRxiv a license to display the preprint in perpetuity. It is made available under aCC-BY-NC-ND 4.0 International license.

Supplemental Table 4. Plasmid table.

Supplemental Table 5. Primer table.

bioRxiv preprint doi: https://doi.org/10.1101/2024.07.28.605507; this version posted August 6, 2024. The copyright holder for this preprint (which was not certified by peer review) is the author/funder, who has granted bioRxiv a license to display the preprint in perpetuity. It is made available under aCC-BY-NC-ND 4.0 International license.

Supplemental Figure 1

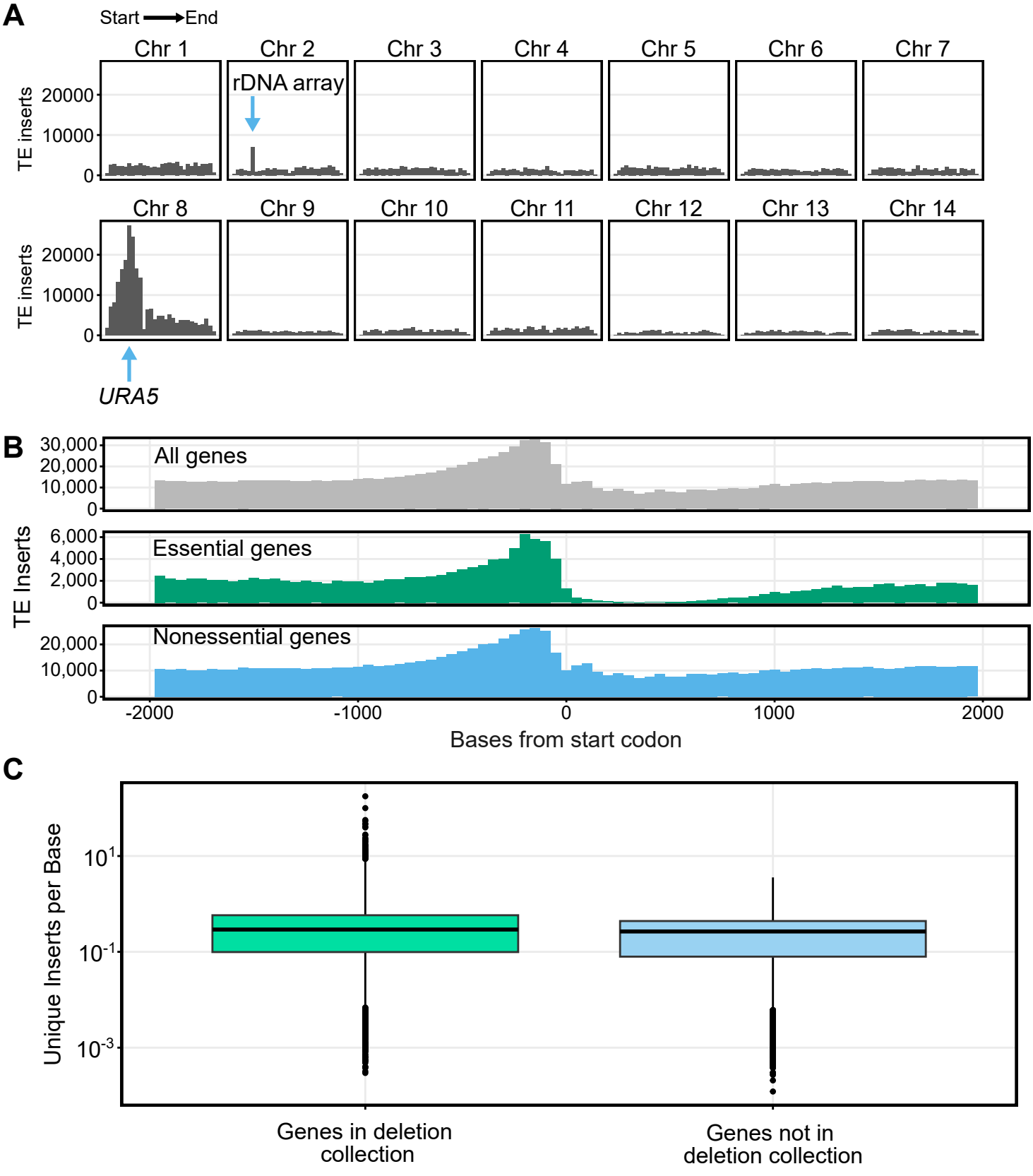

bioRxiv preprint doi: https://doi.org/10.1101/2024.07.28.605507; this version posted August 6, 2024. The copyright holder for this preprint (which was not certified by peer review) is the author/funder, who has granted bioRxiv a license to display the preprint in perpetuity. It is made available under aCC-BY-NC-ND 4.0 International license.

Supplemental Figure 2

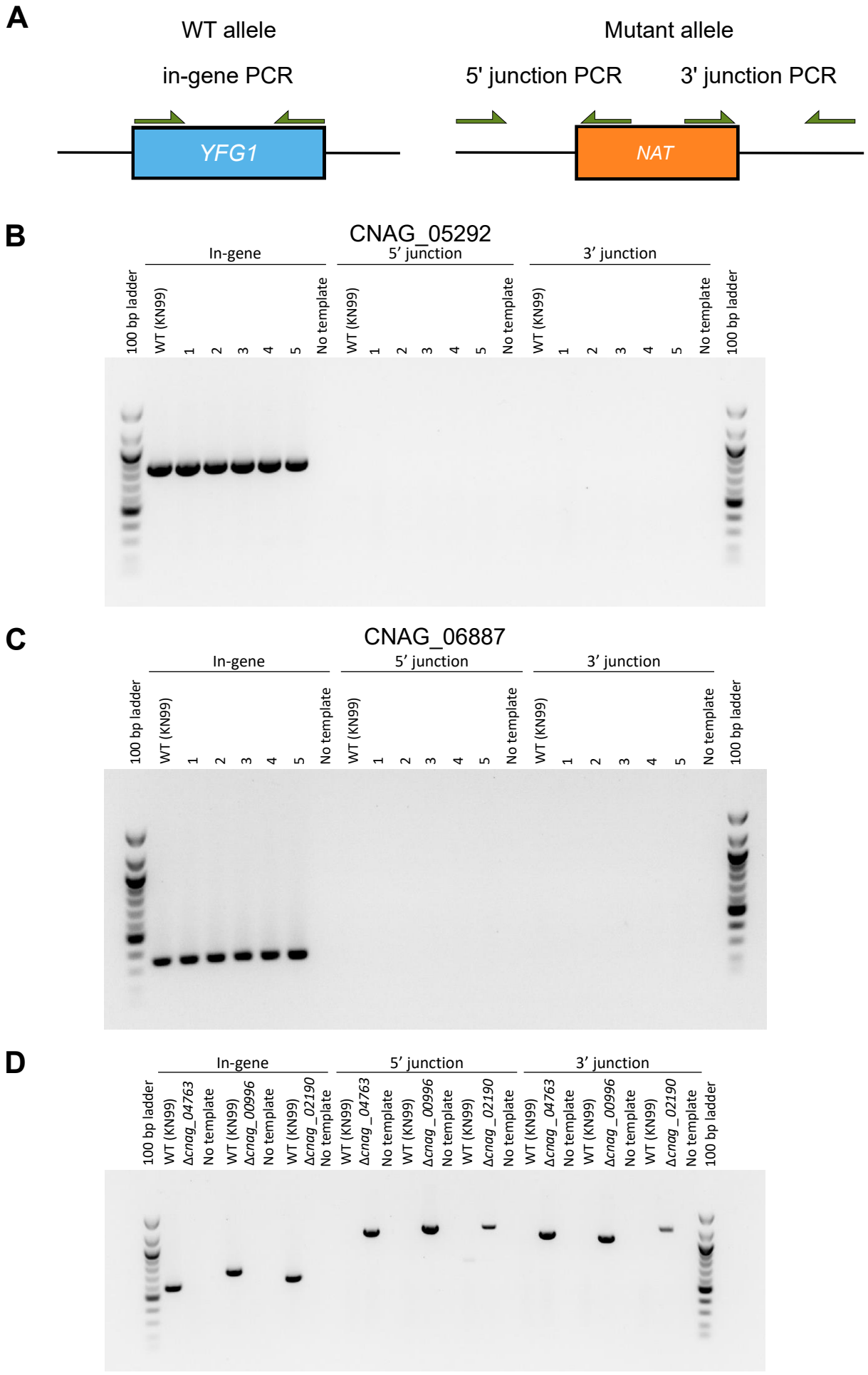

bioRxiv preprint doi: https://doi.org/10.1101/2024.07.28.605507; this version posted August 6, 2024. The copyright holder for this preprint (which was not certified by peer review) is the author/funder, who has granted bioRxiv a license to display the preprint in perpetuity. It is made available under aCC-BY-NC-ND 4.0 International license.

Supplemental Figure 3

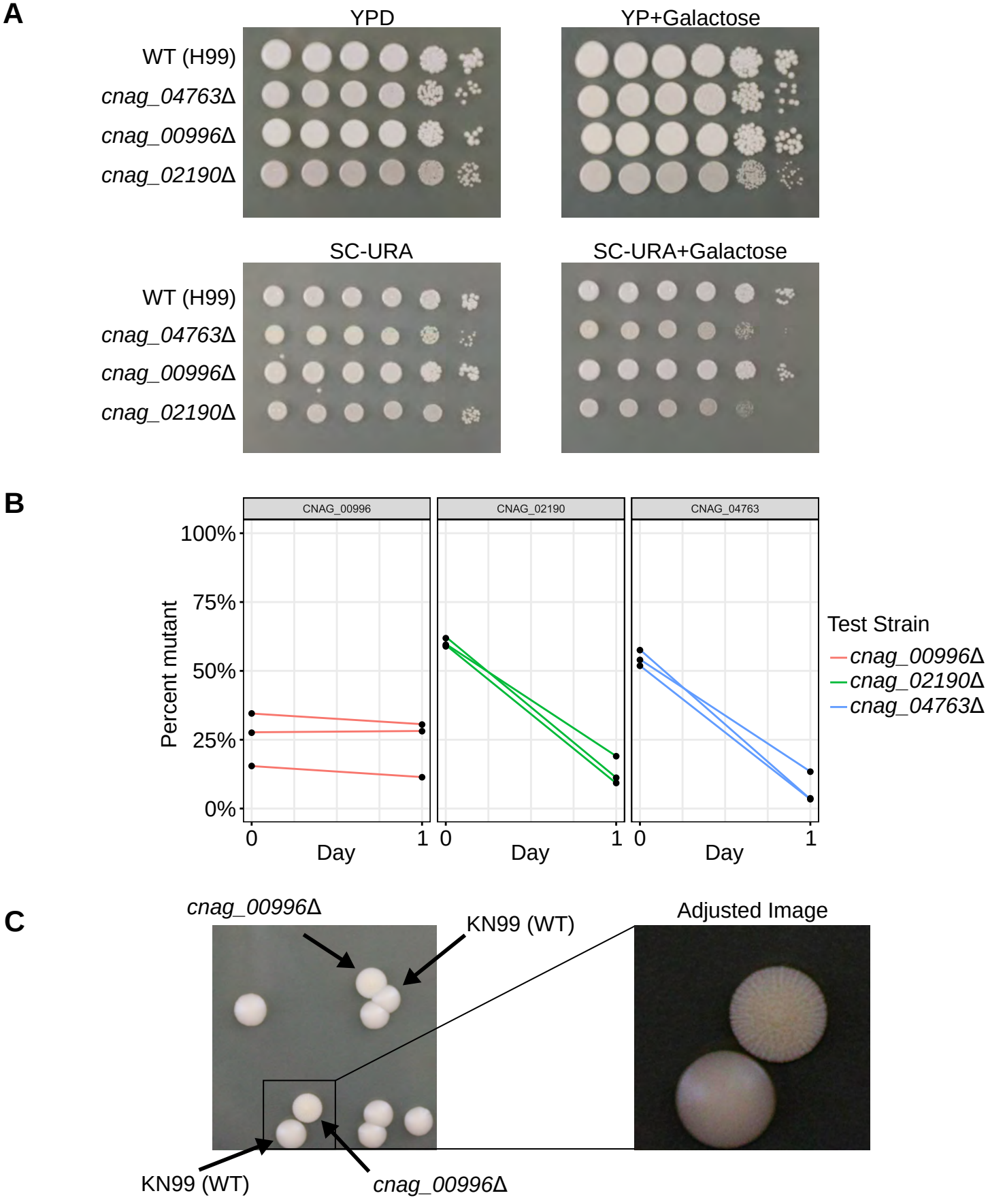

bioRxiv preprint doi: https://doi.org/10.1101/2024.07.28.605507; this version posted August 6, 2024. The copyright holder for this preprint (which was not certified by peer review) is the author/funder, who has granted bioRxiv a license to display the preprint in perpetuity. It is made available under aCC-BY-NC-ND 4.0 International license.

Supplemental Figure 4

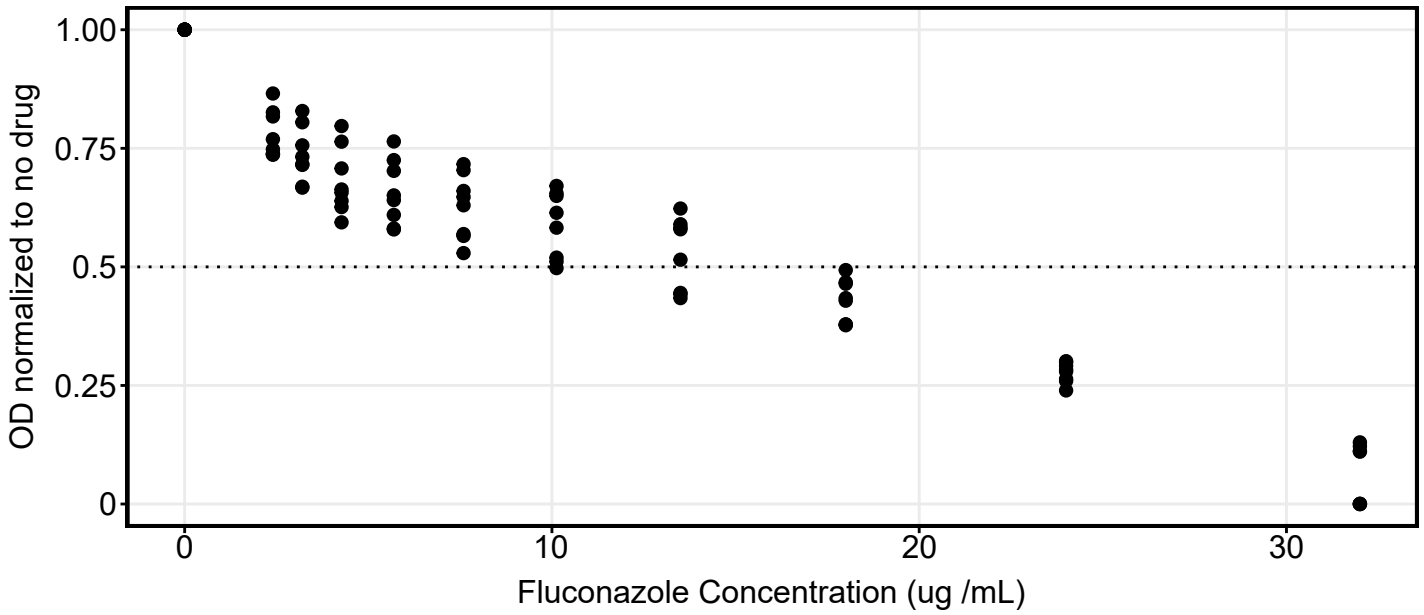

bioRxiv preprint doi: https://doi.org/10.1101/2024.07.28.605507; this version posted August 6, 2024. The copyright holder for this preprint (which was not certified by peer review) is the author/funder, who has granted bioRxiv a license to display the preprint in perpetuity. It is made available under aCC-BY-NC-ND 4.0 International license.

Supplemental Figure 5

Crypto TN-seq

Gene Name:

CNAG_05431

Link to FungiDB